J Mater Sci (2007) 42:7579–7585
DOI 10.1007/s10853-006-1448-y

The effects of heat treatment on the mechanical properties of multicomponent white cast irons

A. Ziadi · F. J. Belzunce · C. Rodriguez

Received: 10 March 2004 / Accepted: 13 April 2006 / Published online: 22 June 2007

Abstract Multicomponent white cast irons contain many kinds of strong carbide-forming elements in order to obtain a very hard microstructure characterized by the presence of different carbides that are well dispersed in a martensitic matrix. The heat treatment of these products consists of high temperature austenization followed by quenching and two temperings, as required in order to increase their overall hardness and to completely eliminate residual austenite. The influence of tempering temperatures on the mechanical properties of these products, determined using tensile, hot compression and fracture toughness tests, was studied in this research work. Their corresponding failure micromechanisms were defined by means of the analysis of fracture surfaces.

Introduction

Chromium–nickel alloyed white cast irons are highly demanded products in the mining, mineral processing, metallurgical and cement industries on account of their high hardness and abrasion resistance, obtained from a microstructure characterized by a high content of primary and eutectic carbides dispersed in a tempered martensitic phase [1, 2].

The currently increasing request demand for greater productivity and product quality has led to the development of higher performance materials. Multicomponent white cast irons are new products, manufactured by adding important percentages of carbide-forming elements, such as chromium, vanadium, molybdenum, tungsten, etc, in order to obtain a microstructure composed of carbides with an extreme hardness dispersed in a matrix that still contains a sufficient percentage of carbon to allow a large increase in hardness as a consequence of the complete transformation of austenite into martensite that occurs in a quenching and tempering heat treatment [3]. The shaping of all these products is carried out by means of casting technologies, directly after the elaboration of the alloy in a liquid state. Being hypoeutectic cast irons, their solidification starts with the nucleation of austenite dendrites and then continues with the formation of different eutectic constituents (γ + MC, in high niobium and vanadium castings, $\gamma + M_7C_3$, when they have a high chromium content, $\gamma + M_2C$ and $\gamma + M_6C$, in the case of high tungsten and molybdenum castings). During cooling, significant quantities of these same carbides precipitate as a result of the typical loss in solubility of the austenite as the temperature is reduced.

The heat treatment of these products consists in austenitization at a high enough temperature so as to dissolve most of the carbides that had precipitated in the previous cooling. A high-alloyed austenite with high carbon content is obtained that is partially transformed into martensite by an appropriate quench. However, an important fraction of retained austenite

A. Ziadi
Department of Mechanical Engineering,
University of Sidi Bel Abbes, Sidi Bel Abbes 22000, Algeria

F. J. Belzunce (✉) · C. Rodriguez
Higher Polytechnic School of Engineering,
University of Oviedo, University Campus,
33203 Gijon, Spain
e-mail: belzunce@epsiq.uniovi.es

remains after the hardening treatment that must be completely eliminated by applying two or more tempering heat treatments. In the course of these tempering treatments, a significant structural hardening takes place (secondary hardening) that is related to a uniform precipitation of very fine carbides, along with the transformation of retained austenite into martensite. Finally, after two or even three tempering treatments, a final hardness of between 600 and 800 HV can be obtained [4, 5].

Experimental procedure

The chemical composition of the white cast iron used in this work is shown in Table 1.

This cast iron was austenitized, quenched and finally double tempered. Different tempering temperatures were used with the aim of modifying the final hardness of the product within a practical range. Figure 1 shows the typical microstructure of these multicomponent cast irons, characterized by a dendritic tempered martensite phase in a matrix of MC, M_7C_3 and M_6C eutectic carbides.

Figure 2 shows the variation in cast iron hardness with the tempering parameter, $P = T(20 + \log t)$, which takes into account the combined effect of temperature (K) and time (h) of the two tempering treatments. The figure shows the continuous decrease in hardness with the tempering parameter.

Any significant microstructure differences can be appreciated among these four treatments. The main effect of increasing tempering temperature (T_1 to T_4) is the growth of the small carbides that precipitate in the course of this heat treatment.

Tensile, hot compression and fracture toughness tests were carried out on each of these four products. Tensile tests were performed according to ASTM E8M-92 standard on cylindrical specimens with a diameter of 6 mm and a calibrated length of 60 mm, under a strain rate of 1 mm/min.

Hot compression tests were carried out at 500 °C, according to ASTM E9 and E209 standards, on specimens with a diameter and length of 5 mm and a 6 mm, respectively, under a strain rate of 1 mm/min.

Table 1 Chemical composition of the product (% in weight)

%C	%Mn	%Si	%S	%P
1.7–1.9	0.5–07	0.9–1.1	<0.025	<0.025
%Ni	%Cr	%Mo	%W	%V
0.7–0.9	7.5–8.5	3–4	1.5–2.5	4–5

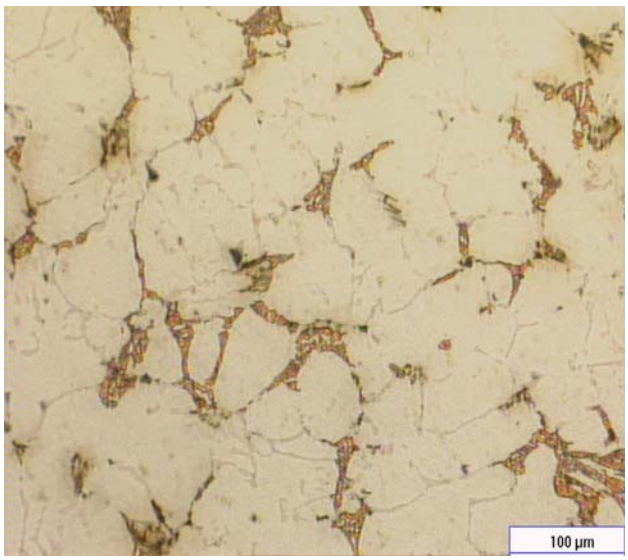

Fig. 1 Microstructure of the heat-treated multicomponent cast iron

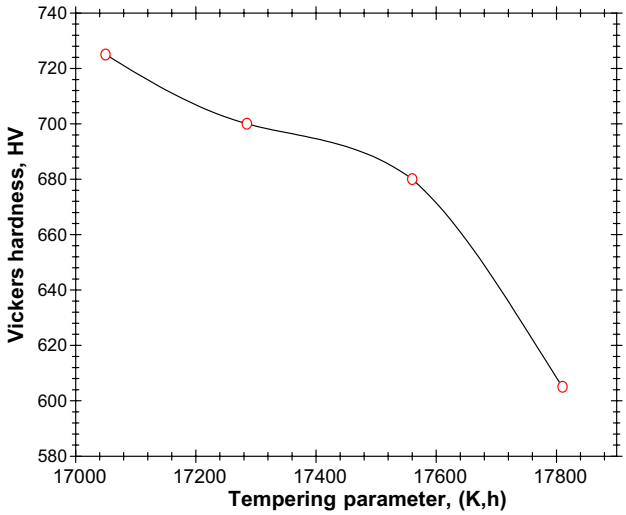

Fig. 2 Evolution of Vickers hardness with the tempering parameter

Specimens extracted in the radial and transverse directions of the product were used. These tests were carried out with the assistance of a furnace equipped with a temperature controller, which was incorporated to the testing machine so as to heat the specimens at a heating rate of 5 °C/min until attaining 500 °C. This temperature was then maintained during 30 min before commencing the compression test. Subsequently, a specimen-less test was carried out under the same conditions to determine the deformation behaviour of the unit blocks and bars used to apply of the load and,

by subtraction, to obtain the real deformation of the specimens.

Finally, the tests for the determination of the fracture toughness were carried out according to ESIS P2-92 and ASTM E399-90 standards on SENB specimens with a cross-section of 15×15 mm. All the specimens were precracked by fatigue, in accordance with the standards.

Results

Tensile tests

Table 2 shows the results of the tensile tests (tensile strength, σ_R, failure elongation, A and reduction of area, Z) along with the Vickers hardness obtained in all these heat treatments. It is worth noting the extremely low ductility of all these products and the significant strength reduction of the white cast iron tempered at the highest temperature (T_4), which also presented the lowest hardness values.

Examination of the failure surfaces of these specimens by SEM always showed an intergranular fracture associated to the carbide network, which constituted the matrix phase of these cast irons (Figs. 3, 4). However, any significant difference was observed among the various heat treatments carried out.

Hot compression tests

The results of the compression tests are shown in Fig. 5 and Table 3 (yield strength, σ_y, compressive strength, σ_R, and deformation at failure, A).

As no important difference was observed between the radial and tangential specimens, the results that are presented in Table 3 refer to the specimens extracted in the radial direction. On the other hand, as mentioned in the experimental procedure, the graphs in Fig. 5 and all the values of deformation at failure, A, were corrected by means of a specimen-less test carried out under the same conditions as the others.

The excellent behaviour that these multicomponent white cast irons displayed in the compression tests carried out at 500 °C is worth noting. This was characterized by very high values of yield and compressive strength, along with a relatively ductile behaviour, as most of these specimens showed plastic deformations at failure higher than 10%. Figure 6, on the other hand, highlights the existing proportionality between the compressive strength at 500 °C and the product hardness measured at room temperature.

Failure of hot compression specimens always took place through a smooth plane located at 45° of the axis of load application, the maximum shear stress plane.

Table 2 Results of the tensile tests

Heat treatment	HV	σ_R (MPa)	A (%)	Z (%)
T_1	725	748	0.30	0.23
T_2	700	782	0.37	0.27
T_3	680	–		–
T_4	605	647	1.00	0.50

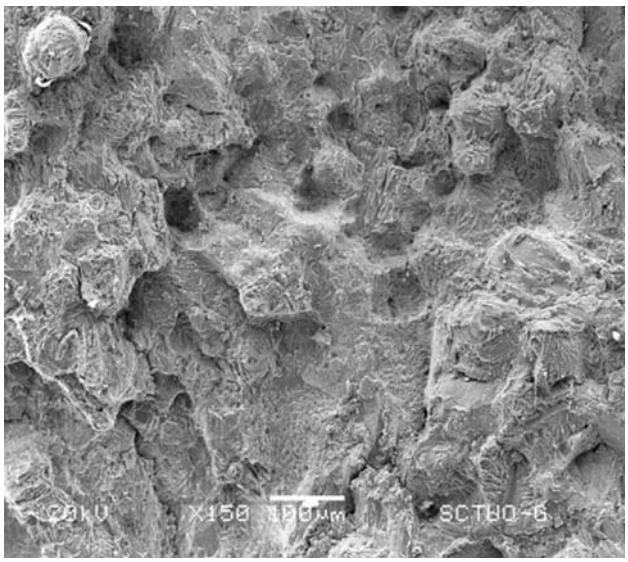

Fig. 3 General pattern of fractured surfaces in the tensile tests (T_2)

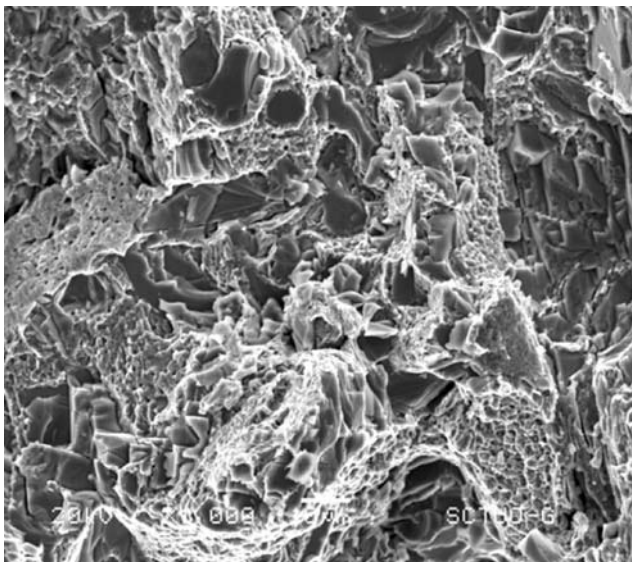

Fig. 4 Detail of the tensile test fractured surface (T_3)

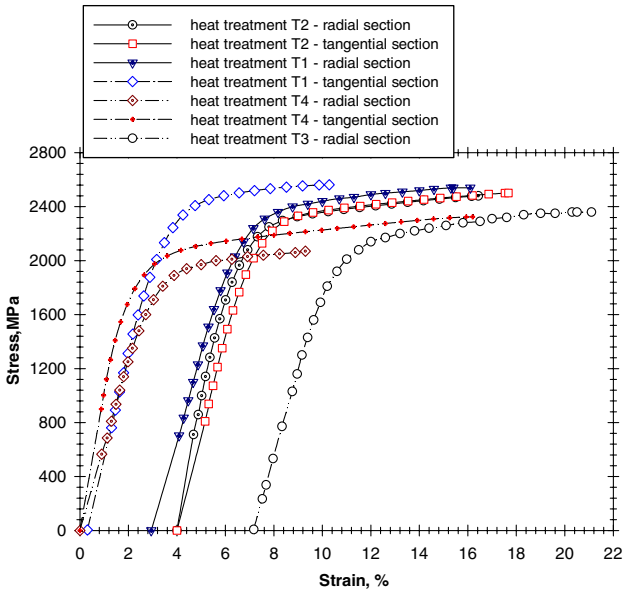

Fig. 5 500 °C compression stress–strain curves once the flexibility of the testing machine and accessories has been corrected

Table 3 Results of compression tests at 500 °C

Heat treatment	HV	σ_y (MPa)	σ_R (MPa)	A (%)
T_1	725	1,982	2,546	12.5
T_2	700	1,800	2,481	13
T_3	680	1,777	2,362	9.5
T_4	605	1,640	2,069	14

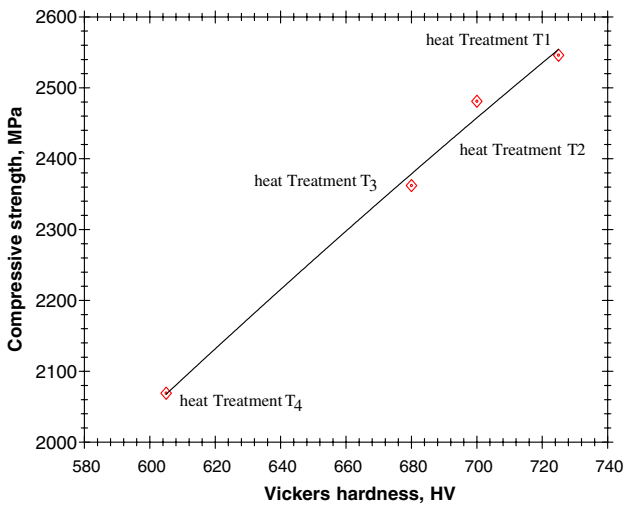

Fig. 6 Relation between Vickers hardness at room temperature and compressive strength at 500 °C

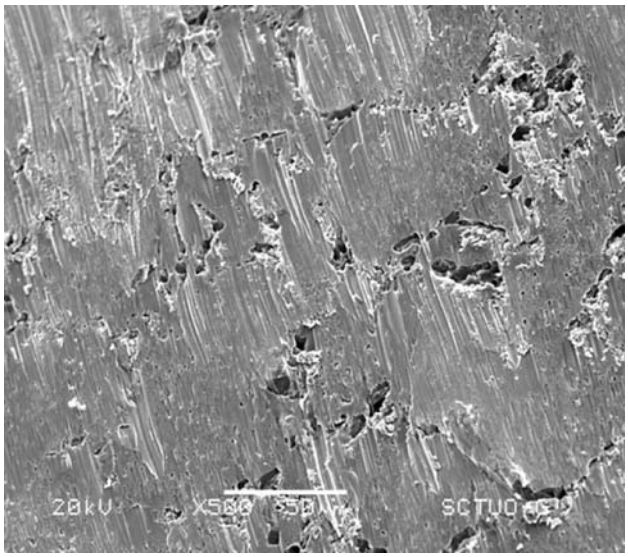

Fig. 7 Typical failure surfaces in 500 °C compression tests

The failure surface, which is presented in Fig. 7, is very flat and shows hardly any characteristic morphological detail, except for large cavities promoted by the growth after debonding of the interphases between carbides and the dendritic globules and also the small microcavities that appear in this last phase as a consequence of the extraction of the very small carbides that had precipitated during the tempering heat treatments.

It is worth noting that the fraction of the failure surface associated with the presence of carbides is clearly lower than that observed on the polished surface. This indicates that hot compression failure took place mainly through the dendritic tempered martensite phase.

The high stiffness and extreme hardness of the carbides present in these microstructures limit their deformation and promote failure along the weakest phase (tempered martensite), although, as already mentioned, the interphase between carbides and martensite is quite weak and decohesion and carbide extraction also occurs in the course of the failure process.

Fracture toughness tests

The tests to determine the fracture toughness of multicomponent cast irons always gave rise to linear elastic behaviours, characterized by the sudden rupture of the precracked specimens when a critical value of the stress intensity factor was attained. As can be seen in Table 4, all the tests were carried out under plane deformation and restricted plasticity conditions, it thus

Table 4 Fracture toughness test results

Heat treatment	HV	K_Q (MPa√m)	P_{max}/P_Q	$B > 2.5 (K_Q/\sigma_y)^2$
T_1	725	28	1.00	YES
T_2	700	29	1.00	YES
T_3	680	26	1.00	YES
T_4	605	26	1.00	YES

being possible to determine the fracture toughness of all these products ($K_Q = K_{Ic}$).

The fracture toughness of this white cast iron hardly varies with heat treatment, although a slight increase in this property was observed when increasing the hardness of these products via heat treatment. On the other hand, it is interesting to note the high fracture toughness values of these multicomponent white cast irons compared with the values assigned by the technical literature to conventional martensitic white cast irons, which are in the range 14–20 MPa√m [6, 7].

Figure 8 shows the general failure pattern of these specimens. As was also revealed in the tensile tests, failure is predominantly intergranular, through the carbide network, (see also Fig. 3). The fractographic detail of Fig. 9 shows the intergranular character of the failure of all these specimens more clearly: an almost continuous carbide network that ruptured in a brittle

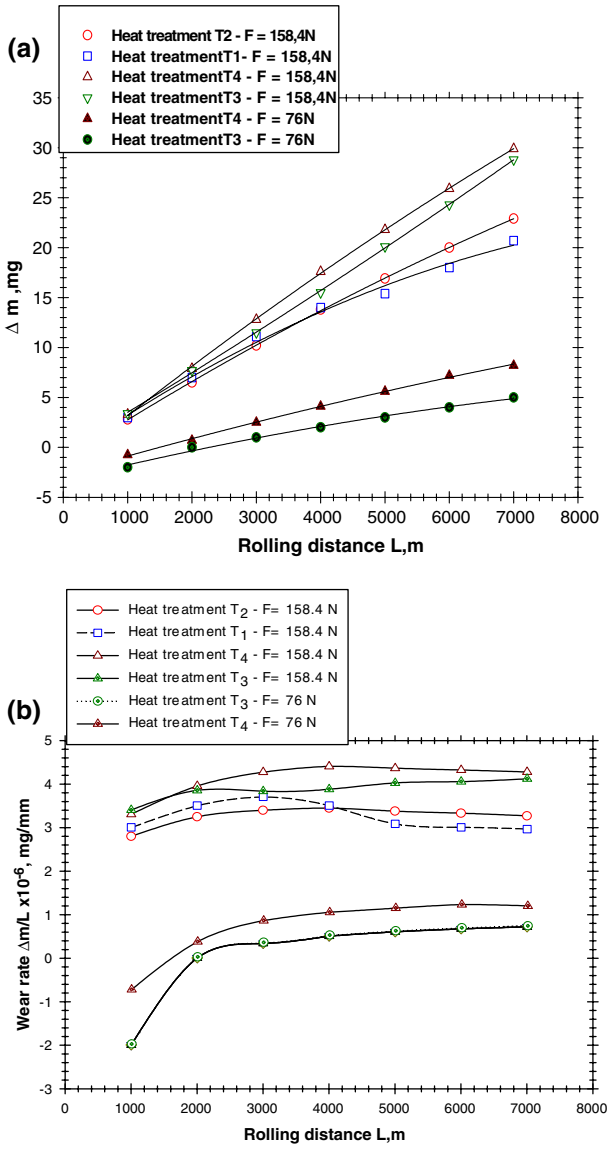

Fig. 8 General fracture pattern of the cast irons in the toughness tests

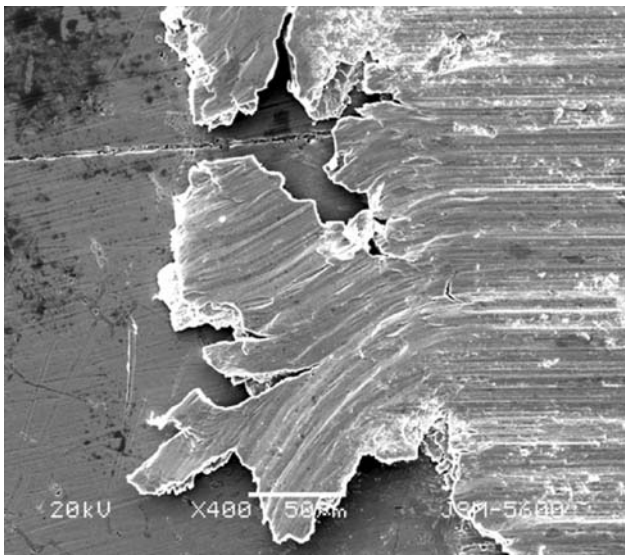

Fig. 9 Fracture toughness test surface detail

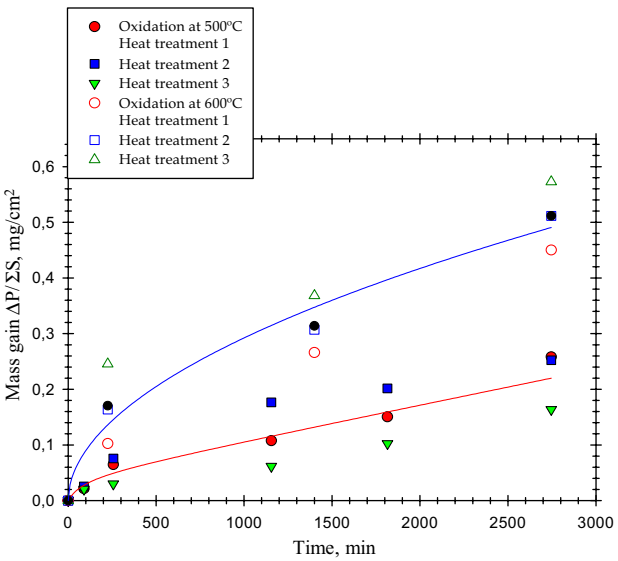

Fig. 10 Oxidation curve

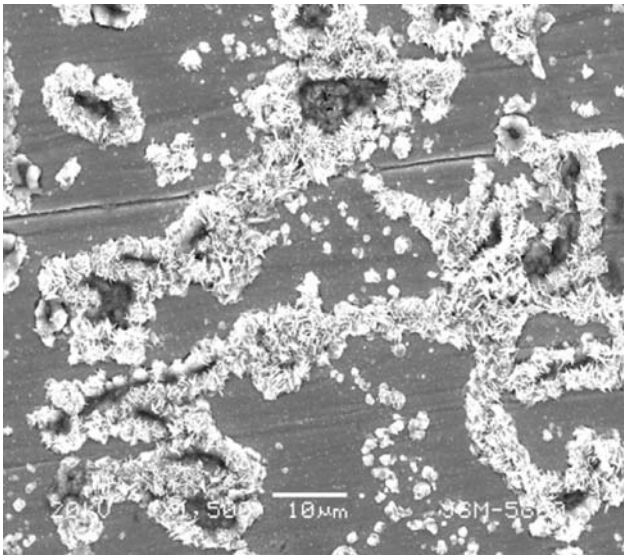

Fig. 11 Oxide morphology–oxidation at 500 ºC

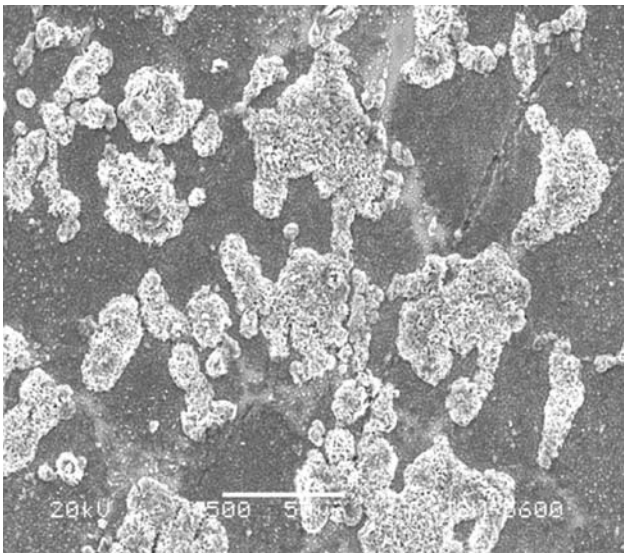

Fig. 12 Oxide morphology–oxidation at 600 ºC

way (cleavage fracture) is seen, with very visible secondary cracks, where the debonding of the carbide/martensite interphase can also be noted. The dendritic phase (tempered martensite), which normally appears isolated (discontinuous areas) in these fractographs, presents a great number of microcavities, giving it the appearance of a ductile failure.

Intergranular brittle fracture due to cleavage or debonding of the eutectic carbides, which constitute the matrix phase of this cast iron (see Fig. 1) is the most characteristic feature. Similar to the findings of other authors [7–9], and in contrast to what was observed in the hot compression tests, the fraction of carbides on these broken surfaces is clearly larger than that measured on polished surfaces, indicating preferential crack progression along these brittle phases.

On the other hand, the regions of ductile appearance (microcavities smaller than 1 μm) are generated when the crack, as it progresses, crosses the dendritic tempered martensite areas. These are tougher regions that, although not being able to stop the cracks, at least make their normal propagation difficult.

On the other hand, the presence of microcavities in the regions of ductile appearance is the result of initial decohesion and subsequent extraction of the small spherical carbides that have precipitated in these regions in the course of the tempering treatments.

The small decrease in fracture toughness observed in the case of the higher tempering temperatures (T_3 and T_4 treatments) may be attributed to the presence of larger precipitated carbides (carbides grow during tempering), giving rise to larger microcavities. Some authors [10] report that the presence of secondary carbides is negative from the white cast iron fracture toughness point of view due to dislocation movement inhibition, although a second reason to explain this experimental fact may be that these carbides facilitate the propagation of the cracks by means of their decohesion with the parent phase.

Conclusions

The present study of the variation of the mechanical behaviour of a multicomponent white cast iron with the tempering heat treatment (hardness modification) led to the following conclusions:

- After an appropriate heat treatment, these cast irons are very hard products whose tensile strength decreases along with their hardness on increasing the tempering time and temperature.
- The 500 °C hot compression behaviour of these cast irons is excellent: their strengths are very high and their ductilities normally exceeds 10%, a linear relation having been obtained between their compressive strength at 500 °C and their room temperature hardness.
- The fracture toughness of these cast irons is relatively high, especially when we compare it with that of conventional white cast iron with similar microstructures. Moreover, this property is hardly modified in the course of normal heat treatments.
- Failure of these products in tensile and fracture toughness tests is intergranular, since it preferentially takes place through the carbide network, due

to their brittleness, and also as a result of the interphase decohesion between carbides and the dendritic tempered martensitic phase, which occurs under the strong local stresses, that developed ahead of the crack front. In contrast, failure of the dendritic areas is ductile in appearance, characterised by the presence of a great number of microcavities generated by virtue of the decohesion of small carbides precipitated during the tempering heat treatments.

Acknowledgements The authors would like to thank the FICYT foundation of the Principado of Asturias for the financing of the research project (project number: PC-CIS-1-14) and also Fundicion Nodular S.A., the company that elaborated the material used in this study.

References

1. Tabrett CP, Sare IR (2000) J Mater Sci 35:2069
2. Zhang MX, Kelly PM, Gates JD (2001) J Mater Sci 36:3865
3. Matsubara Y, Hashimoto M (2003) Iron Steel Met 35
4. Hwang LC, Lee S, Lee HC (1998) Mater Sci Eng A254:282
5. Garcia J et al (2002) In: Proceedings of the 39th Rolling Seminar. Ouro Preto, Brasil
6. Bradley WL, Srinivasan MN (1990) Int Metal Rev 35(3):129
7. Zum Gahr KH, Doane DV (1980) Met Trans 11A:613
8. Sare R (1979) Met Tech 6:412
9. Oh H, Lee S, Jung JY, Ahn S (2001) Met Mater Trans 32A:515
10. Tabrett CP, Sare IR, Ghomashchi MR (1996) Int Mater Rev 41(2):59